International Journal of Hydrogen Energy 216 (2026) 153582

Contents lists available at ScienceDirect

International Journal of Hydrogen Energy

journal homepage: www.elsevier.com/locate/he

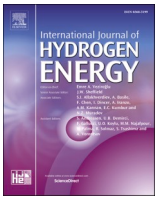

Simulation of the refuelling process for an LH_2-Powered commercial Aircraft: Part 2 - Refuelling time of the Airbus ZEROe turboprop concept

L. ten Damme [a], M. van Put [b], A. Gangoli Rao [a,*]

[a] Faculty of Aerospace Engineering, Delft University of Technology, the Netherlands
[b] Airbus Netherlands B.V, the Netherlands

A B S T R A C T

Liquid hydrogen (LH_2) is gaining momentum as a sustainable aviation fuel, but its cryogenic nature poses significant challenges for ground operations, particularly aircraft refuelling. This process is increasingly recognised as a potential bottleneck for operational efficiency, as it can significantly extend turnaround times. Although some recent studies have proposed assumptions about LH_2 refuelling rates, their conclusions vary widely, and detailed modelling efforts remain limited.

This paper presents the second part of a two-part study that aims to improve understanding of the LH_2 refuelling by delivering a validated numerical modelling framework and practical insights to support the design of future LH_2-powered aircraft and their airport refuelling operations. Part 1 focused on developing and validating a thermodynamic model that captures key physical phenomena such as heat transfer and droplet dynamics. The model was validated against experimental data from the LH_2 no-vent filling tests to demonstrate its accuracy in predicting relevant physical processes.

In Part 2, the validated model is applied to a representative case study based on the Airbus ZEROe Turboprop concept. The objective is to quantify the refuelling time and hydrogen venting under realistic conditions. The simulation results indicate a refuelling time of approximately 19, min and ventilation losses of 36.7, kg, corresponding to approximately 2. 2 % of the total transferred LH_2 mass.

Although the duration of refuelling exceeds that of current kerosene-powered aircraft such as the Bombardier Q400, the overall turnaround time remains feasible if the LH_2 refuelling process is carried out in parallel with other ground operations, subject to safety protocols. These findings challenge simplified assumptions in the previous literature and provide physics-based insight to support the design of safe and efficient LH_2 fuelling procedures and infrastructure for future zero-emission aviation.

Nomenclature

Abbreviations		
Al	aluminium	
EI	emission index	
GH_2	gaseous hydrogen	
LH2	liquid hydrogen	
REFPROP (NIST)	Reference Fluid Thermodynamic and Transport Properties Database	
RT	receiving tank	
SAF	sustainable aviation fuel	
ST	stationary tank	
Symbols		
λ	valve state	–
$\%_{fill}$	fill fraction	–
$\dot{Q}$	rate of heat transfer	W
$\dot{W}$	rate of work	W
ρ	density	$\frac{kg}{m^3}$
$D_{\lambda tr}$	transfer line valve diameter	m
D	diameter	m

(*continued on next column*)

(*continued*)

Abbreviations		
J	mass flow rate	$\frac{kg}{s}$
K	loss factor	–
L	length	m
m	mass	kg
p	pressure	Pa
$\dot{q}''$	heat flux	$\frac{W}{m^2}$
$r_{top-to-bottom}$	ratio between top and bottom fill	–
T_s	temperature of the saturated film	K
T	temperature	K
Subscripts		
avg	average	
l	liquid	
RT	receiving tank	
ST	stationary tank or supply tank	
tr	transfer line	
vap	vaporisation	
vent	vent line	
v	vapour	
w	tank wall	

* Corresponding author.

https://doi.org/10.1016/j.ijhydene.2026.153582
Received 2 January 2025; Received in revised form 22 August 2025; Accepted 15 January 2026
Available online 9 February 2026

1. Introduction

This paper is the second part of a two-part study on the numerical simulation of liquid hydrogen (LH_2) refuelling for commercial aircraft. The general objective of the study is to develop and apply an accurate numerical model to better understand and optimise the LH_2 refuelling process, with particular attention to its thermal and operational aspects.

Part 1 presented the development and validation of a detailed thermodynamic model for LH_2 transfer. The model accounts for key physical phenomena, including heat transfer and droplet evaporation, and was validated against recent experimental data to demonstrate its accuracy in predicting relevant physical processes.

In this second part, the validated model is applied to a representative case study involving a future LH_2-powered commercial aircraft. The aim is to evaluate the refuelling time and assess its effect on overall aircraft turnaround operations. Additionally, the study examines how key operational parameters influence refuelling performance.

The analysis begins with the selection of a case aircraft and the definition of the relevant properties of its refuelling system. These parameters serve as input for the simulation based on the model established in Part 1.Fig. 1

The refuelling process from the trailer to the aircraft tank is then simulated. A schematic of the system is shown in Fig. 2. LH_2 is transferred using pressurised gaseous hydrogen (GH_2), which is generated within the trailer by vaporising a portion of stored LH_2. This process increases the GH_2 pressure and creates a pressure difference that drives the LH_2 into the aircraft tank. By regulating the vaporiser and, thus, the GH_2 pressure, the LH_2 flow rate can be controlled. If the pressure in the trailer or aircraft tank exceeds acceptable limits, hydrogen is vented through dedicated vent lines. LH_2 is delivered to the aircraft tank either directly at the bottom or through a spray inlet at the top.

Finally, a sensitivity analysis is performed to identify the parameters that have the greatest influence on refuelling time. The analysis also investigates how these parameters affect the amount of hydrogen that is vented from the aircraft tank.

2. Airbus ZEROe turboprop concept

In September 2020, Airbus unveiled a series of hydrogen-powered aircraft designs known as the ZE- ROe concepts, as illustrated in Fig. 3. These designs reflect the increasing commitment of the aviation industry to zero-emission alternatives, in response to growing concerns about carbon emissions and their impact on the climate. Each concept incorporates hydrogen-based propulsion as the core technology for enabling carbon-neutral flight.

Hydrogen offers substantial environmental benefits compared to Sustainable Aviation Fuels (SAFs), which are also considered a promising alternative to reduce emissions in aviation. Table 1 compares the Lower Heating Value (LHV) and emission indices (EI) of conventional Jet A-1 (kerosene), various blends of SAF, and liquid hydrogen. In particular, hydrogen does not emit CO_2, soot, or sulphates upon combustion, while producing significantly more water vapour. These properties highlight hydrogen's potential to enable zero-emission flight, provided that contrail management and water vapour impacts are addressed.

According to Ryan and Philip [4], Airbus identifies the Turboprop configuration as the most feasible near-term solution to achieve its goal of introducing a zero-emission aircraft by 2035. Given current technology readiness levels and range requirements, the turboprop is seen as the most viable configuration for early hydrogen-powered commercial aviation. Consequently, this study adopts an aircraft based on the ZEROe Turboprop concept as the baseline for the analysis.

2.1. Comparison with bombardier Q400

Since the technical details of the Airbus ZEROe aircraft proposal are not yet known, a conventional aircraft of similar type is used to derive the characteristics of the proposed ZEROe turboprop aircraft. The Bombardier Q400, a conventional regional turboprop aircraft, is considered the most suitable reference for the Airbus ZEROe Turboprop concept in terms of passenger capacity and range. Although the Q400 can accommodate up to 78 passengers, it has a range of 1,360, NM when carrying 70 passengers [6]. This performance is of the same order of magnitude as that of the Airbus ZEROe Turboprop concept, which is designed for fewer than 100 passengers and a range exceeding 1000 NM, as illustrated in Fig. 3. The Bombardier Q400 has a refuelling time of 6 min [7].

According to Brouwer and Srinivasan [8], a Q400 performing a 300 NM mission would require approximately 1200 kg of kerosene. This implies a fuel consumption per nautical mile as calculated in Eq. (1).

$$\frac{1,200\ kg}{300\ NM} = 4\frac{kg}{NM} \tag{1}$$

The original Bombardier Q400 turboprop aircraft has a maximum seating capacity of 78 passengers. However, in 2018, Bombardier introduced an updated 90-seat variant, first delivered to SpiceJet, an Indian budget airline [9]. Given that the Airbus ZEROe Turboprop is anticipated to enter service by 2035, it is assumed that the Q400 would be able to accommodate 90 passengers while maintaining the same total fuel consumption as its original 78-passenger version. This assumption is supported by historical improvements in fuel efficiency; as illustrated in Fig. 4, the fuel consumption for short-range aircraft (in litres per 100 km per seat) has decreased from approximately 5.5 L in 1980 to 2.8 L in 2018, corresponding to a 49.2 % reduction over 48 years.

By fitting a second-order polynomial trendline to the historical data spanning from 1980 to 2018 and extrapolating this trend to the year 2035, the predicted fuel consumption further decreases to approximately 2.44 L per 100 km per seat. Given that the Bombardier Q400's maiden flight occurred on January 31, 1998 [6], this projected improvement corresponds to an estimated fuel-consumption reduction

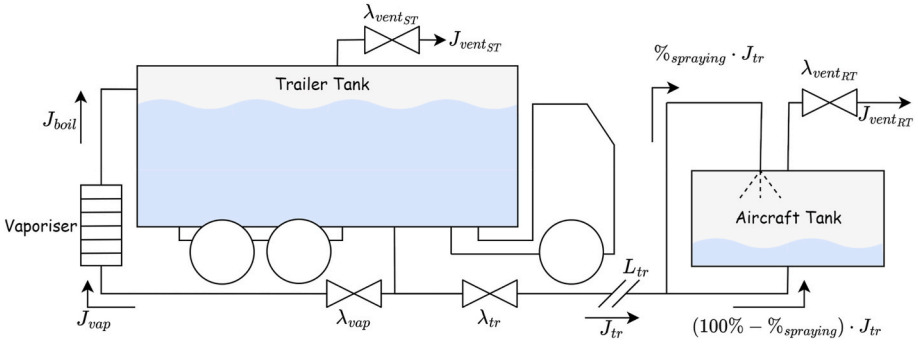

Fig. 1. Schematic of the LH_2 transfer between trailer and aircraft tank of the case study.

Fig. 2. Airbus ZEROe concepts [5].

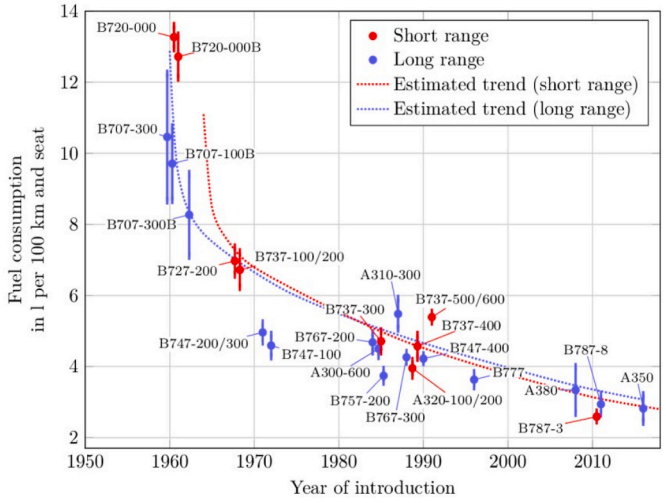

Fig. 3. Evolution of fuel consumption for both small and long-range aircraft [10].

Table 1
Fuel properties and emission indices for different fuel types [1–3].

Property	Jet A-1	50 % SAF	100 % SAF	Hydrogen
LHV [MJ/kg]	43.15	43.6	44.2	119.93
EI CO_2 [kg CO_2/kg]	3.16	1.58	0.00	0.00
EI H_2O [kg H_2O/kg]	1.26	1.32	1.36	8.93
EI Soot [kg/kg]	4.0×10^{-5}	2.0×10^{-5}	0.00	0.00
EI SO_4 [kg/kg]	$2.0\ 10^{-4}$	$1.0\ 10^{-4}$	0.00	0.00

of around 37.3 % by 2035. This significant reduction comfortably exceeds the proposed seating capacity increase of 15.5 % (from 78 to 90 seats). Thus, the assumption that the Q400 could increase its seating capacity while maintaining constant total fuel consumption is considered justified.

Considering a passenger capacity of 90 and the Lower Heating Value (LHV) of Jet A-1 of 43.15 MJ/kg.

(see Table 1), the specific energy consumption per nautical mile (NM) per passenger is calculated according to Eq. (2).

$$4\frac{kg}{NM}\cdot\frac{1}{90Pax}\cdot 43.15\frac{MJ}{kg} = 1.92\frac{MJ}{NM\cdot Pax} \tag{2}$$

As shown in Fig. 5, the adjusted energy consumption for an LH_2-fueled equivalent regional propeller aircraft, which is expected to require 14 % more energy, is given in Eq. (3).

$$1.92\frac{MJ}{NM\cdot Pax}\times 1.14 = 2.19\frac{MJ}{NM\cdot Pax}$$

2.2. Energy requirements

The fuel consumption of the calculated Bombardier Q400 equivalent LH_2 aircraft (2.19 MJ/(NM · PAX)) is used to determine the total fuel required. In line with Fig. 3, it is assumed that the range of the ZEROe Turboprop is 1000 NM and the number of seats is 90. The total energy required on board is calculated in Eq. (4).

$$2.19\frac{MJ}{NM\cdot Pax}\times 1000NM\times 90Pax = 196.8\ GJ \tag{4}$$

The LHV of LH_2 is 119 MJ/kg, as listed in Table 1. Based on this LHV, the required mass of LH_2 is calculated in Eq. (5).

$$\frac{196.8\ GJ}{119\frac{MJ}{kg}} = 1640.7\ kg$$

To ensure cryogenic temperatures are maintained during normal operation, it is assumed that a minimum of 5 % of the LH_2 must remain in the tanks. Therefore, the final onboard LH_2 mass is increased accordingly, as shown in Eq. (6).

$$1.05\ \cdot\ 1,640.7\ \text{kg} = 1,722.7\ \text{kg} \tag{6}$$

The norm *NPR-ISO/PAS 15594:2004 Airport hydrogen fuelling facility operations* prescribes LH_2 requirements for various aircraft types [12]. From this list, the TU 334 LH_2 version is considered most in line with the ZEROe Turboprop concept in terms of passenger capacity and range. The TU 334 has a maximum of 102 seats and a maximum range of 1101–1544 NM, depending on the variant [6].

The operating pressure of the tank is assumed to be between 1.2 and 2 bar. The LH_2 density in the aircraft tank is taken at the maximum operating (venting) pressure of 2 bar, where it reaches a value of 67.7 $\frac{kg}{m^3}$ [13]. A gas layer must always be present above the liquid phase in the tank, which means that the tank cannot be completely filled with liquid. Therefore, the maximum fill fraction is assumed to be 95 %, which leads to a correction factor as given in Eq. (7).

$$\frac{1}{0.95} = 1.053 \tag{7}$$

According to Fig. 6, the LH_2 is assumed to be stored in two identical

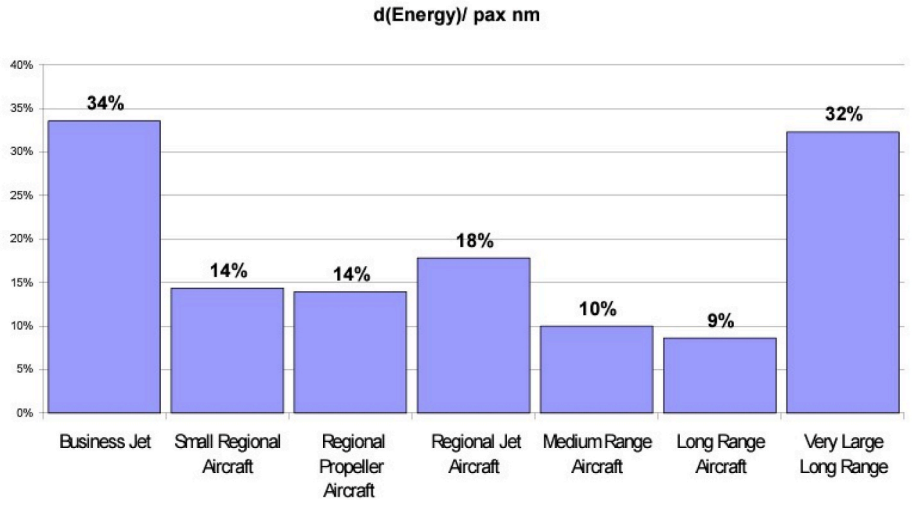

Fig. 4. Change of energy consumption for LH_2 aircraft compared to conventional aircraft [11].

Fig. 5. LH_2 tanks in Airbus ZEROe Turboprop concept [14].

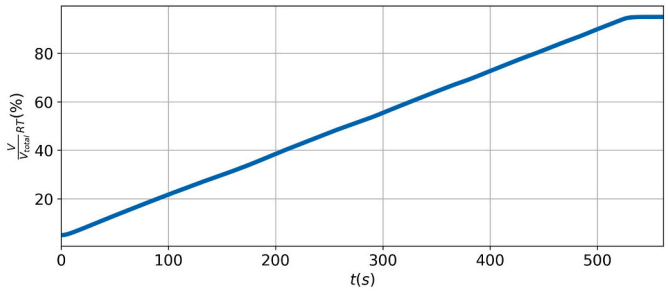

Fig. 6. Fill level in receiving tank.

tanks. The volume per tank is determined in Eq. (8).

$$\frac{1,7227kg}{0.95 \cdot 67.7 \frac{kg}{m^3} \cdot 2} = 13.4m^3 \tag{8}$$

2.3. Aircraft cryogenic tank

As mentioned above, the operational pressure is considered to be 1.2−2 bar and the maximum fill level is 95 %. The initial pressure is set to 1.2 bar and the initial liquid temperature is set to 20 K, which is slightly lower than the saturation temperature of 20.86 K at 1.2 bar. In addition, it is assumed that there is only bottom-filling, and thus no spraying. The initial liquid temperature is set to 20 K. Finally, it is assumed that the two tanks are refuelled serially, implying that the final refuelling time is double the refuelling time of a single tank.

The tanks are assumed to be horizontal-orientated cylinders. According to Ref. [6], the Bombardier Q400 has a maximum fuselage diameter of 2.69 m. It is assumed that the fuselage diameter of the ZEROe Turboprop concept is approximately the same. However, to accommodate factors such as tank wall thickness, insulation, maintenance space, and placement, a margin is considered. Therefore, the inner tank diameter is estimated to be 2 m, resulting in a length of 4.3 m per tank.

A standardised hose size diameter must be considered for future LH_2 refuelling that must be suitable for different sized aircraft to reduce investment cost for airports. The norm *NPR-ISO/PAS 15594:2004 Airport hydrogen fuelling facility operations* prescribed that: *"manual coupling units used for the refuelling and boil-off management operations of small aircraft"* shall have a connector diameter of 30 mm or 1.18 inch, while *"mechanized coupling units used for the refuelling and boil-off management operations of large aircraft"* shall have a connector diameter of 140 mm or 5.5 inch [12]. The same norm also stated that:" The *quantity of LH_2 to be refuelled prior to each flight ranges from* 410 kg *for a small aircraft,* 6700 kg *for a medium aircraft, and up to* 33,000 kg *for a large aircraft.* As the total LH_2 onboard of the case study aircraft is calculated to be 1722.7 kg, the aircraft is considered more in line with a small aircraft. Therefore, it is assumed that the orifice diameter is 30 mm. The tank wall is assumed to be 5 mm.

The material categories allowed for cryogenic vessels (vacuum insulated) (EN 13458-2) include aluminium and stainless-steel alloys due to their well-established cryogenic application, high strength-to weight ratio, and superior corrosion resistance [15,16]. Aluminium alloys are preferred over stainless steel in aircraft applications due to their higher strength-to-weight ratio. The chosen specific aluminium alloy is 5083-O and the aluminium 5083-O density is 2650 $\frac{kg}{m^3}$

A constant heat flux from the environment to the tank wall of 10 W/m^2 is assumed, as this value has been validated against experimental data for a ground-based cryogenic LH_2 tank in Ref. [17]. In addition, since it is assumed that the system stays cold due to the leftover 5 % LH_2

in the tank, the initial temperatures of the wall connected to the vapour and liquid are considered equal to the initial temperatures of the vapour and liquid respectably.

2.4. Infrastructure

The transfer line is assumed to be 10 m. Again, *NPR-ISO/PAS 15594:2004 Airport hydrogen fuelling facility operations* prescribe that manual coupling units used for the refuelling and boil-off management operations of small aircraft must have a diameter of 30 mm. Therefore, it is assumed that both the transfer line and its valve diameter are 30 mm. Consistent with the analysis in Part 1 of this study, the transfer line roughness is assumed to be 1 μm. Additionally, the same loss factor ($K = 11$) is adopted, given that the pipe diameters considered here (25.4 mm and 30 mm) are approximately equal. Following the methodology established in Part 1, the refuelling process is considered complete once the flow rate within the transfer line drops below $1 \cdot 10^{-3}$ kg/s.

An LH_2 trailer from Hylium Industries, Inc. is considered, for which the most important specifications of interest are listed in Table 2. Using the schematics, the outer volume of the trailer is calculated to be 58.7 m^3, while the capacity of the trailer is specified as 40,000–48,000 L. Assuming a representative capacity of 44 m^3, a geometric scaling factor is applied to account for the difference between the inner and outer dimensions. This scaling factor is calculated in Eq. (9).

$$\sqrt[3]{\frac{44}{58.7}} = 0.908 \tag{9}$$

The trailer is simplified to a horizontal cylinder, neglecting the semi-elliptical heads or end caps. It is assumed that the LH_2 inside the trailer is in a saturated state. Furthermore, the maximum fill fraction is assumed to be 90 %, resulting in a payload of 2529 kg at 3 bar_g. The operational pressure is defined as 3 $bar_g \pm 5$ %, and it is assumed that the initial liquid temperature is equal to the saturation temperature at the lowest operational pressure.

As with the aircraft tank, it is assumed that the diameter of the orifice is 30 mm.

In addition, it is assumed that a vaporiser is present in the trailer, operating at the saturation temperature corresponding to 3 bar_g. The vaporiser valve coefficient must be high enough to allow adequate mass flow into the vaporiser to ensure proper operation.

2.5. Simulating the refuelling process

Using the tank model developed and validated in Part 1 of this study, which captures key physical processes such as heat transfer and droplet evaporation, the refuelling process of a case study aircraft similar to the Airbus ZEROe Turboprop concept was simulated. An overview of the assumptions and key parameters is shown in Table 3. A complete list of model inputs used for the case study is provided in Table 5.

2.6. Sensitivity analysis

It is of interest to examine which input parameters have the greatest influence on fuelling time. In addition, it is relevant to analyse how modifying those input parameters affects the amount of venting from the aircraft tank. To do so, a sensitivity analysis is performed. This section discusses the selected parameters along with the values for which their influence is analysed.

First, a slightly subcooled initial temperature of 20 K is considered in the aircraft tank. In addition, an even lower temperature of 19 K and a saturation temperature of 20.86 K are evaluated. Next, it is assumed that the ventilation pressure is 2 bar, based on *NPR-ISO/PAS 15594:2004 Airport hydrogen fuelling facility operations* [12]. However, Brewer and Boeing considered venting pressures of 1.4 bar and 2.5 bar, respectively. Therefore, the effect of these alternative venting pressures on the refuelling process is also examined.

Since the heat ingress into the tank strongly depends on insulation system, tank geometry, and ambient conditions, variations in heat ingress are considered by evaluating ±25 % and ±50 % of the assumed baseline of 10 W/m^2.

As mentioned earlier, two identical tanks are assumed. Based on Fig. 6, these tanks are placed sequentially in the aft section of the fuselage, similar to conventional aircraft. As a result of this

Table 2
Specifications of the LH_2 trailer [18].

Capacity	40,000 − 48,000 L
Kind of fluid	LH_2
Payload	2500 − 3000 kg
Design pressure	10.0 bar_g
Operating pressure	3.0 bar_g
Design temperature	−253-38 °C
Operating temperature	−253-38 °C
Insulation	Multi-layer insulation & vacuum insulation
Normal evaporation rate	0.9 % per day

Table 3
Overview of assumptions and key parameters used in the ZEROe Turboprop case study.

Parameter	Value	Type
Comparison with Bombardier Q400		
Range	1000 NM	Assumption
Passenger capacity	90 PAX	Assumption
Fuel consumption (LH_2 equivalent)	2.19 NMMJ·PAX	Derived
Total energy required	196.8 GJ	Computed
Energy Requirements		
LHV Jet A-1		Reference
LHV LH_2	43.15 $\frac{MJ}{kg}$ 119.93 $\frac{MJ}{kg}$	Reference
LH_2 density (2 bar)	67.7 m_kg3	Reference
Reserve margin	5 %	Assumption
Total LH_2 mass incl. reserve	1722.7 kg	Computed
Scaling factor trailer volume	$\sqrt[3]{\frac{44}{58.7}} = 0.908$	Computed
Aircraft Cryogenic Tank		
Tank fill fraction	95 %	Assumption
Number of tanks	2	Assumption
Tank volume (per tank)	13.4 m^3	Computed
Tank inner diameter	2.0 m	Assumption
Tank length	4.3 m	Computed
Wall thickness	5.0 mm	Assumption
Tank material	Aluminium 5083-O	Assumption
Material density	2650 kg/m^3	Reference
Heat flux	10 W/m^2	Assumption
Initial liquid temperature	20K	Assumption
Initial vapour temperature	20 K	Assumption
Initial tank pressure	1.2 bar	Assumption
Tank fill method	Bottom fill (no spray)	Assumption
Refuelling configuration	Serial (one tank at a time)	Assumption
Infrastructure		
Transfer line length	10 m	Assumption
Transfer line diameter	30 mm	Norm-based
Transfer line roughness	1 μm	Assumption
Loss factor (K)	11	Assumption
Flow cut-off (refuelling ends)	$1 \cdot 10^{-3}$ kg/s	Assumption
LH_2 Trailer		
Trailer geometry	Horizontal cylinder (no end caps)	Simplification
LH_2 state in trailer	Saturated	Assumption
Maximum fill fraction (trailer)	90 %	Assumption
Payload at 3 bar_g	2529 kg	Computed
Trailer volume	44 m^3	Assumption
Operating pressure	3 ± 5 % bar_g	Assumption
Initial liquid temperature	Saturation temp at lowest pressure	Assumption
Vaporiser temperature	Saturation temp at 3 bar_g	Assumption

configuration, the tanks have different transfer line lengths. To assess the effect of this variation, the impact of modifying the baseline length of 10 m by ±25 % and ±50 % is analysed.

The cryogenic tank material is assumed to be aluminium, which is commonly used for vacuum-insulated vessels due to its high strength-to-weight ratio. However, the influence of using stainless steel instead of aluminium is also considered.

The diameter of the transfer line is selected according to the same norm, which states that type 1 coupling units used to refuel small aircrafts must have a diameter of 30 mm. However, type 2 coupling units for larger aircraft have a diameter of 140 mm. Therefore, the effect of using a Type 2 connector on refuelling time and venting behaviour is investigated.

Two different analyses are performed concerning the loss factor (K-factor) of the connector. In the first analysis, the same loss factor ($K = 11$) as for the type 1 connector is assumed. As explained previously in Part 1 of this study, the loss factor represents the flow resistance through a component. Although the relationship between component diameter and loss factor generally follows a negative logarithmic trend, a conservative linear reduction is adopted here for simplicity. The scaling ratio between the connector diameters is given by Eq. (10).

$$\frac{140mm}{30mm} = 4.67 \tag{10}$$

The reduced loss factor is then calculated in Eq. (11).

$$\frac{11}{4.67} = 2.36 \tag{11}$$

The effect of this modified loss factor on the refuelling process is also analysed when using a type 2 connector.

Next, the influence of different wall temperatures inside the aircraft tank is examined. Since no two-phase boiling heat transfer correlations are implemented in the current model, wall temperatures of 30 K and 40 K are considered. These imply excess temperatures of approximately 10 K and 20 K, respectively. According to Darr et al. [19], the onset of nucleate boiling already occurs at an excess temperature of 2 K. Therefore, the current heat transfer model does not accurately capture the physics at these higher excess temperatures. However, their impact on refuelling time and venting behaviour is still analysed, acknowledging that the actual heat transfer would likely be higher in reality due to two-phase boiling.

The thickness of the aircraft tank wall is initially assumed to be 5 mm. This value is not based on a specific structural analysis. To examine the sensitivity to this assumption, the deviations of ±2 mm are considered. Onorato (2021) [16] investigated fuel tank designs for various LH_2 aircraft and found that the wall thickness of a non-integral tank for an ATR72, a comparable aircraft to the ZEROe Turboprop concept, was 2.5 mm. This suggests that the baseline assumption of 5 mm is conservative.

The effect of spray filling (top fill) on the refuelling process is also analysed. Numerous experimental studies have shown that spray filling significantly reduces refuelling losses. It is therefore of interest to assess whether this trend holds in the simulation model. The influence of spraying on both refuelling time and venting is evaluated for spray percentages of 0 %, 25 %, 50 %, 75 %, and 100 %.

Refuelling is assumed to occur serially. This implies that the refuelling time and venting of one tank are simply doubled to obtain the total values for both tanks. However, the effect of parallel refuelling is also considered. In that case, although only one filling line is used, the mass flow rate through the transfer line is divided by two.

The considered LH_2 refuelling trailer from Hylium Industries, Inc. has an operating pressure of 3 bar_g, as listed in Table 2. The impact of using a trailer with higher operating pressure is also examined. Specifically, the operating pressure increases from 1 bar to 4 bar_g.

Finally, as previously discussed in Section 2.1, the comparison with the Bombardier Q400 relies on the assumption that the fuel consumption for the 90-seat variant remains equal to that of the original 78-seat version. Consequently, the sensitivity analysis also evaluates the impact of this assumption on the refuelling time and hydrogen venting behaviour.

All parameters and corresponding values used in the sensitivity analysis are summarised in Table 4.

3. Results

The results of the case study are provided in this section. First, the results from simulating the refuelling process for the case aircraft are presented in Section 3.1. Next, the results of the sensitivity analysis, as described in Section 2.6, are presented in Section 3.2.

3.1. Simulating the refuelling process for the case aircraft

The refuelling time for the case aircraft, similar to the Airbus ZEROe Turboprop concept, is simulated as 18 min and 43 s. This is more than three times longer than the refuelling time of the kerosene powered equivalent, the Bombardier Q400. The amount of venting from the aircraft tank is found to be 36.7 kg, which is 2.24 % of the total transferred mass. The computational time is 38 min and 43 s.

As shown in Figs. 7 and 12, the fill level and the amount of LH_2 in the receiving tank increase approximately linearly, with some deviation near the end of the refuelling process. Fig. 10 shows the behaviour of the transient temperature in the aircraft tank, revealing that the temperature of the wall lags behind the temperature changes of the liquid and hydrogen of the vapour due to the thermal inertia of the wall.

As mentioned in Section 2.2, the norm *NPR-ISO/PAS 15594:2004*

Table 4
Relevant parameters and values for the sensitivity analysis of the case study.

Parameter	Symbol	Unit	Value
Initial liquid temperature in aircraft tank	$Tl,RTt = 0$	K	19 20 20.86
Venting pressure in aircraft tank	$pvent,RT$	bar_a	1.4 2 2.5
Heat ingress in aircraft tank	q''_{RT}	$\frac{W}{m2}$	5 7.5 10 12.5 15
Transfer line length	L_{tr}	m	5 7.5 10 12.5 15
Material of the aircraft tank	RT tank material		Al5083 SS304
Transfer line diameter	D_{tr}	m	30 $140K = 11$ $140K =$ 2.36
Initial wall temperature of the aircraft tank	Tw,RT	K	$Tv,lt = 0$ 30 40
Wall thickness of the aircraft tank	tw,RT	mm	3 5 7
Percentage of spraying in aircraft tank	Spray	%	0 25 50 75 100
Refuelling method in aircraft tank	Method		Serial Parallel
Operating pressure in refuelling trailer	pST	bar_g	3 4
Number of passengers considered for the Bombardier Q400	Bombardier Q400	PAX	78 90

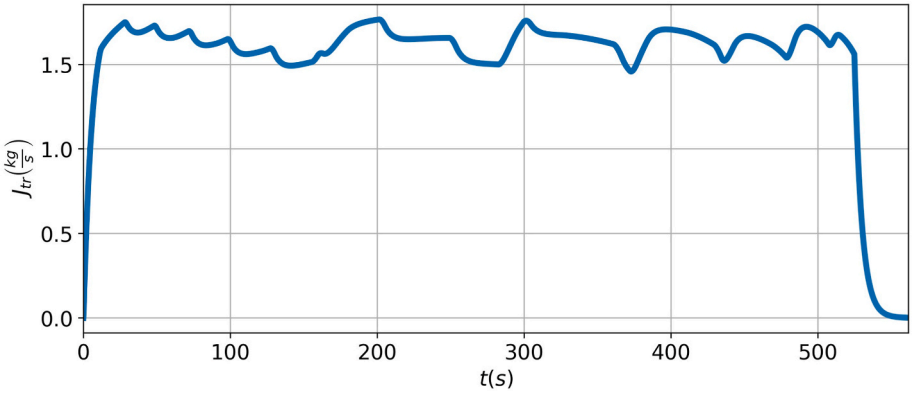

Fig. 7. Mass flow rate in transfer line.

Airport hydrogen fuelling facility operations prescribes LH_2 requirements for different types of aircraft, where the TU 334 LH_2 version is considered most in line in terms of passengers and range. It states that the refuelling block time is 20 min and the estimated flow time is 15 min for a total fuel amount of 1100 kg. The total mass of liquid onboard the case study aircraft is found to be 1722.7 kg. For simplified comparison, the average flow speed of the norm is 1.22 kg/s. As shown in Fig. 8, the average flow speed obtained from the simulation for the case study aircraft is slightly higher, at 1.53 kg/s Nonetheless, the flow rates can be regarded to be of the same order of magnitude.

In Figs. 9 and 11, it can be observed that both the duration of vent valve openings and the interval between consecutive venting events decrease over the course of the refuelling process. This trend is attributed to the reduction in the vapour volume as the amount of LH_2 in the aircraft tank increases. As a result of venting, the mass of GH_2 in the receiving tank decreases, as shown in Fig. 13. As the interval between venting events shortens, the maximum temperature of the vapour, as shown in Fig. 10, gradually decreases.

The maximum vaporiser flow rate is 0.30 kg/s, as shown in Fig. 14. With an enthalpy of vaporisation in the trailer tank of 390$\frac{kJ}{kg}$, the required vaporiser power is 117 kW. The selected immersion heater, a 120 kW, 6inch model, meets the criteria and fits within the trailer tank [20]. It requires 480 V and three phase electric power. The calculated total energy needed for the vaporiser during the 18 min and 43 s refuelling time is 36.5 kWh, which is comparable to the capacity of a small electric vehicle battery and could be accommodated on a separate trailer.

In Fig. 15, the minimal increase in tank pressure observed after refuelling indicates that heat ingress has a limited effect on the dynamic behaviour of the hydrogen within the tank during this period. However, it is important to note that this model does not account for thermal stratification, which could potentially result in a more pronounced pressure increase under real-world conditions.Table 5

3.2. Sensitivity analysis

The results of the sensitivity analysis, detailed in Table 4, examine the impact of various parameters on fuelling times and losses. The results, normalised with respect to the refuelling case as prescribed in Section 2.5, are summarised in Table 6. The results of the sensitivity analysis are discussed in detail here.

The initial liquid temperature in the aircraft tank had minimal impact on refuelling time and losses. Slight reductions in refuelling time are noted with higher temperatures, although losses increased slightly. Heat ingress similarly had negligible effects on both refuelling time and losses.

Venting pressure significantly influenced the refuelling time. Reducing the venting pressure to 1.4 bar led to a 7 % decrease in refuelling time, while increasing it to 2.5 bar resulted in a 6 % increase. A decrease in the venting pressure by 0.1 bar reduced the refuelling time by approximately 1.2 %.

For LH_2, the liquid density decreases as the saturation pressure increases. As the tank size in the model is based on the liquid density at the venting pressure, a higher venting pressure leads to a lower liquid density. This requires a larger refuelling tank to store the same amount of energy. This relationship probably explains why higher venting pressures are associated with longer refuelling times.

The length of the transfer line also had a notable effect. Increasing the length by 25 % resulted in a 6 % increase in refuelling time, attributable to greater pressure drops and reduced mass flow rates. Switching the tank material from aluminium to steel did not have a significant impact, which confirms the advantage of aluminium due to

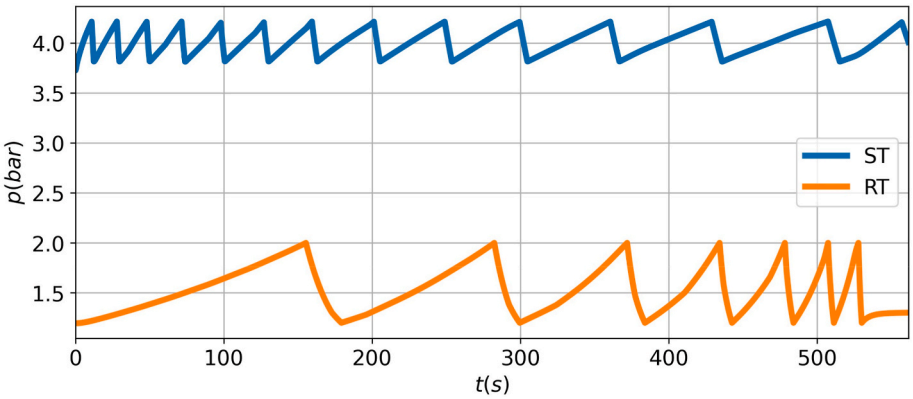

Fig. 8. Pressure in the stationary tank (ST) and the receiving tank (RT).

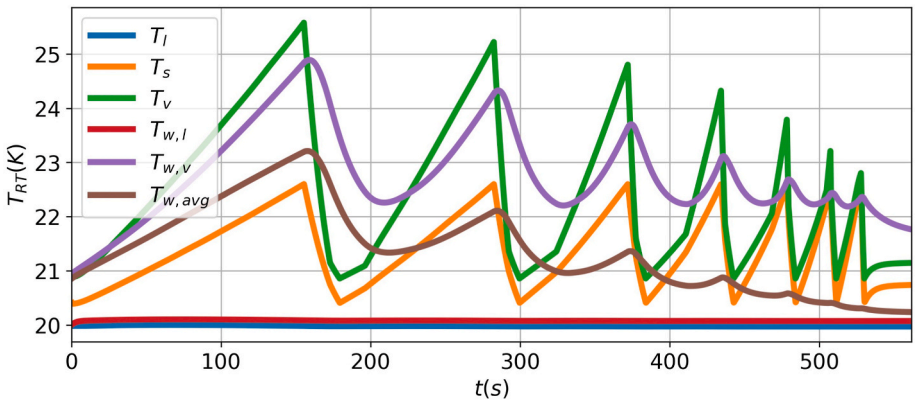

Fig. 9. Temperatures in receiving tank.

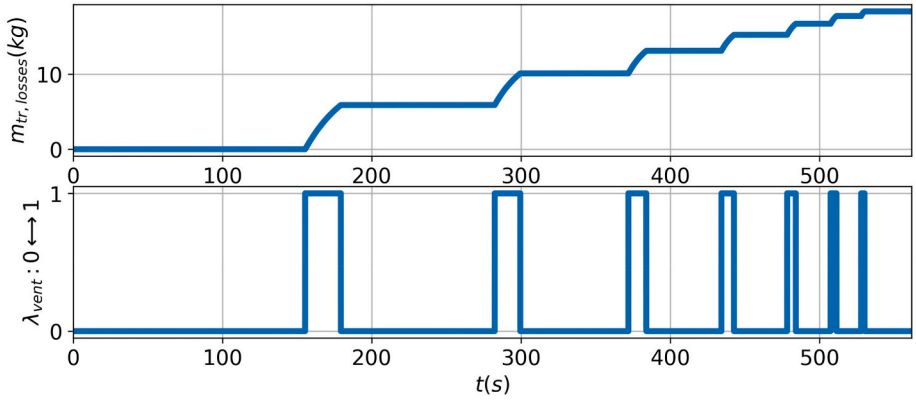

Fig. 10. Venting from the receiving tank.

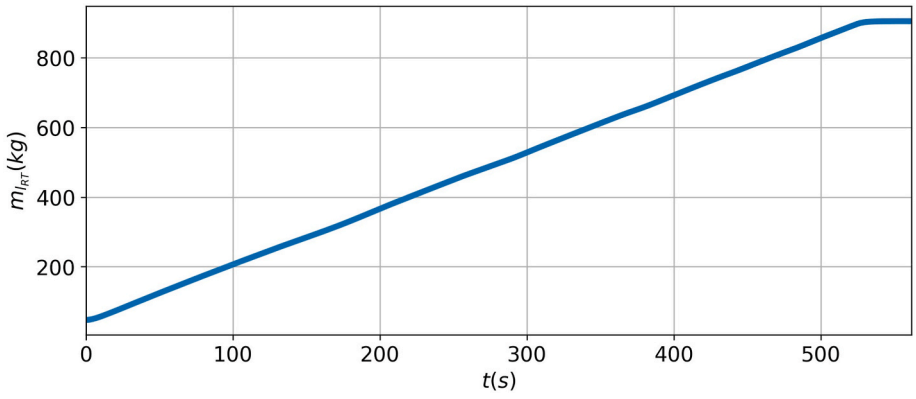

Fig. 11. Liquid mass in receiving tank.

its lower mass. However, increasing the diameter of the transfer line from 30 mm to 140 mm is the most effective way to reduce refuelling time, as it increased the mass flow rate. The associated increase in the coefficient of the vaporiser valve and the power requirements requires further consideration for the design and integration of the aircraft system.

The initial wall temperature of the tank had a minor effect on the refuelling time, with a slight reduction in ventilation observed at 30 K. This effect is expected to be even smaller in practice due to two-phase heat transfer, which would cause faster cooling of the tank wall. The thickness of the wall did not show a significant effect, as the tank wall is already chilled down, rendering the increase in thermal mass insignificant.

Increasing the percentage of spraying in the aircraft tank significantly reduced venting but also raised the liquid temperature, potentially leading to two-phase flow issues. When pumps are used to pump the LH_2 from the tank to the engines, the two-phase flow could result in cavitation of the pump. Cavitation is undesired, as significant damage could occur to the pump. Therefore, more research is needed to assess the impact of spraying on pump cavitation. Parallel refuelling is found to shorten refuelling times by 2 % and reduce venting by 3 % compared to serial refuelling, likely due to the reduced time required to close the supply tank valve.

Increasing the operating pressure in the refuelling trailer by 1 bar resulted in a 14 % reduction in refuelling time and a small 2 % decrease in venting. This reduction is attributed to the increased pressure drop.

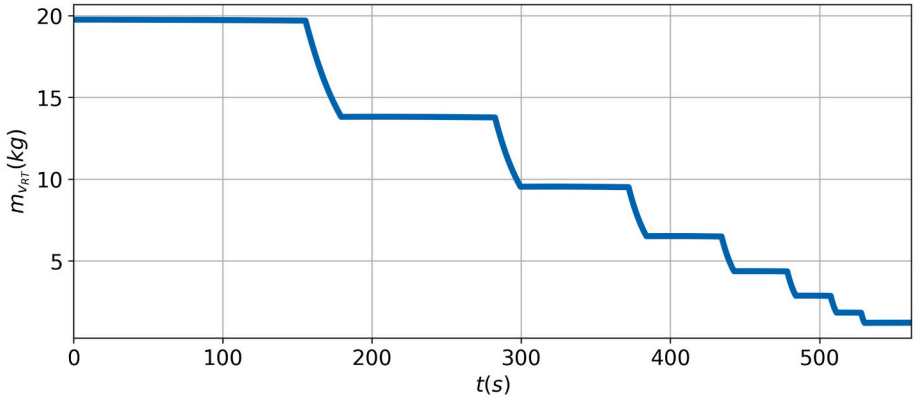

Fig. 12. Vapour mass in receiving tank.

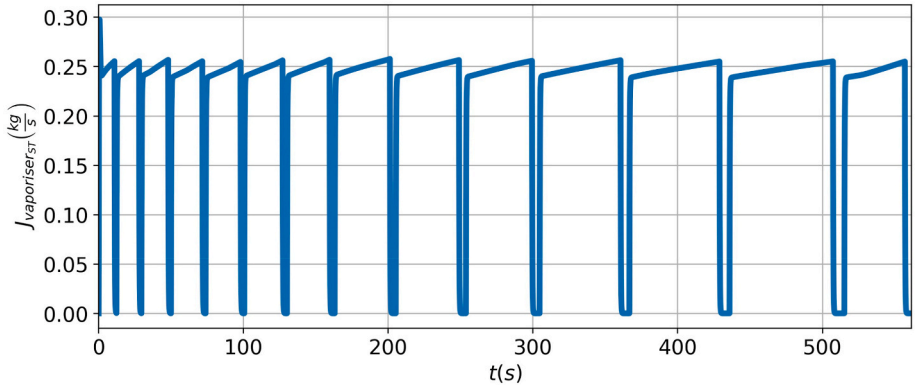

Fig. 13. Mass flow rate in the boiler.

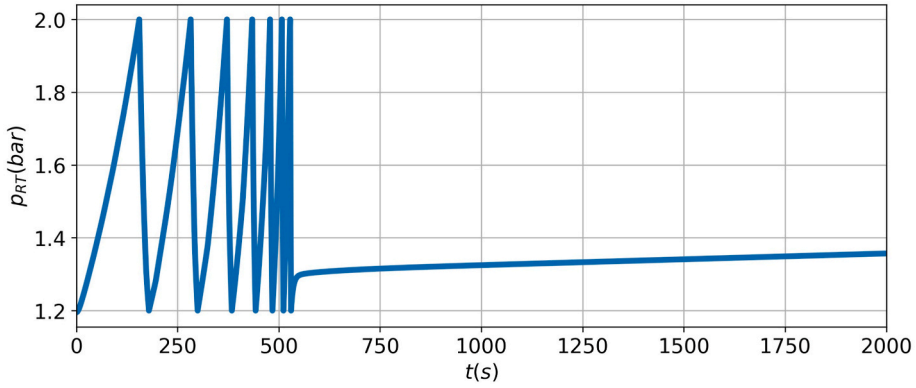

Fig. 14. Pressure variation in the aircraft tank during a period of 2000 s after the start of the filling process.

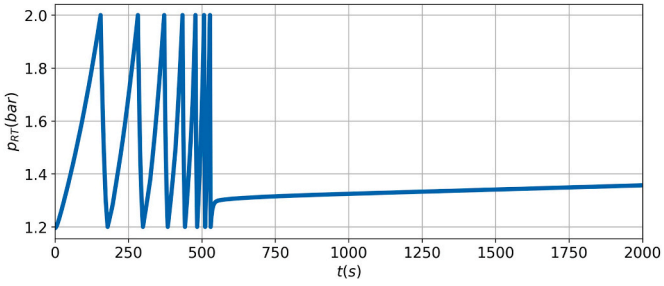

Fig. 15. Time required for each step of the LH_2 refuelling process [21].

Lastly, for the Bombardier Q400, increasing the number of seats from 78 to 90 led to a 14 % increase in refuelling time and a 15 % increase in venting, assuming current fuel consumption rates.

4. Discussion and conclusions

A case study simulating the refuelling process for a commercial aircraft similar to the Airbus ZEROe Turboprop concept is conducted. The validated tank model, as presented in the preceding paper, simulated a refuelling time of approximately 19 min. This duration exceeds the refuelling time of a kerosene-powered equivalent aircraft by more than a factor of three.

Mangold et al. [21] evaluated the duration required for each individual step involved in the normal refuelling process of LH_2 aircraft

Table 5
Model inputs for the case study.

A. Model Input			
General	Value	Transfer Line	Value
fluid	REFPROP::PARAHYD	Dtr	3.00E-02
p_atm	1.01E+05	Ltr	10.00
T_amb	288.00	drtr	1.00E-06
g	9.81	tau_tr	5.00
psiToPa	6894.76	dE	3.00E-02
T_c	32.94	kE	11.00
p_c	1.32E+06	Aircraft Tank	Value
Lambda	5.00	ZEROe_tanks	2.00
DD	6.00E-03	VTotal2	13.39
Dti_DD	0.80	tw2	5.00E-03
nL1	11.00	R2	1.00
tminL1	0.10	Lcyl2	4.26
nL2	11.00	p20	1.20E+05
tminL2	0.10	Tv20	20.94
nV1	11.00	TL20	20.00
tminV1	0.10	TwL20	20.00
nV2	11.00	Twv20	20.94
tminV2	0.10	pct_VL20	0.05
tStart	0.00	Ts20	20.41
tFinal	2000.00	VL20	0.67
relTol	1.00E-04	hL20	0.19
Trailer Tank	Value	rhoL20	70.15
VTotal1	44.00	mL20	46.98
R1	0.94	rhov20	1.55
A1	2.75	mv20	19.74
Lcyl1	16.00	ratio_top_bottom	0.00
p10	4.01E+05	Qdotconstant2	10.00
TL10	25.71	rho_tank	2650.00
Tv10	26.07	mw2	355.83
rhov10	4.85	MaterialTank2	Aluminum5083
rhoL10	63.32	S_valve2	7.07E-04
pct_VL10	0.90	ETVentState	0.00
totalmass10	2528.78	p_ET_low	1.20E+05
Vullage10	4.40	p_ET_high	2.00E+05
mL10	2490.09	TopET	0.95
mv10	21.36		
Ts10	25.98		
Jboil0	0.00		
Jtr0	0.00		
Qdotconstant1	1.02		
mVap0	0.00		
Tboil	25.97		
tau_vap	0.20		
c_vap	8.00E-05		
VapValveState	0.00		
S_valve1	7.07E-04		
STVentState	0.00		

during ground turnaround. As illustrated in Fig. 15, most of these process steps have durations independent of the quantity of hydrogen being refuelled; only the actual LH_2 refuelling step is directly influenced by the transferred amount. When incorporating these additional procedural steps, the total LH_2 refuelling time is approximately 28 min.

During the refuelling process, the amount of vented liquid hydrogen from the aircraft tank is calculated to be 36.7 kg, which constitutes 2.2 % of the total transferred LH_2. The aircraft design used in the case study is based on assumptions, as detailed information about the Airbus ZEROe is not yet available. The results therefore represent a first estimation and should be interpreted with appropriate caution.

Several key factors influenced the refuelling time, including the venting pressure of the aircraft tank, the operational pressure in the trailer tank, and the length and diameter of the transfer line. A 25 % increase in transfer line length resulted in a 6 % increase in refuelling time. In contrast, a reduction in venting pressure by 0.1 bar led to a 1.2 % decrease in refuelling time. Notably, the spraying percentage in the aircraft tank is identified as the most significant factor affecting venting; 100 % spraying reduced venting by 30 %.

The refuelling time for the Airbus A320 is approximately 12 min. Despite the A320's larger seating capacity and extended range, its total turnaround time is 48 min, which is 20 min longer than the simulated refuelling time for the case study aircraft. Consequently, if LH_2 refuelling can be integrated into other turnaround tasks, the calculated refuelling duration would be well in time to meet turnaround constraints. This conclusion is in line with the findings of Mangold et al. [21], who argued that the LH_2 refuelling procedure does not negatively impact aircraft turnaround times. It is important to note, however, that if refuelling cannot be performed in parallel with other tasks, this may lead to extended turnaround durations, negatively affecting aircraft utilisation and profitability. Hence, the integration of refuelling within operational procedures remains a critical factor in overall airline economics.

Also, some other points of discussion are identified. Firstly, according to the standard *NPR-ISO/PAS 15594:2004*, the average flow speed for an equivalent LH_2 aircraft is 1.22 kg/s. The simulated average flow speed for the case study aircraft is slightly higher at 1.53 kg/s. While the standard value is conservative, it is significantly lower than the 20 kg/s suggested by Mangold et al. [21] and the flow rates assumed by Clean Hydrogen Joint Undertaking [22].

Secondly, the current study considered a pressure feed system, as suitable LH_2 pumps are not yet commercially available. However, pump-fed refuelling may become feasible in the near future due to ongoing pump developments. This would allow for higher pressure drops and potentially shorter refuelling durations. To accurately simulate such systems, model modifications will be necessary. In addition, further investigation is required into the capability of vaporiser technology for LH_2 trailers to handle the thermal and flow demands under realistic operating conditions. The practicality of providing the required electrical power, potentially from a separate power trailer, must also be assessed.

Additionally, the simulation assumed identical fuel tanks and a serial refuelling configuration, effectively doubling the refuelling time of a single tank. While this is a reasonable assumption for tanks placed sequentially, future aircraft configurations may use parallel or asymmetrical tank layouts, which would require separate analysis.

Another point of interest is the residual LH_2 inflow observed after closing the supply valve. In practice, the loss of driving pressure results in a pressure surge in the transfer line upon valve closure. The actual closure behaviour of the valve may deviate from the simulation assumptions, indicating a need for further investigation into valve dynamics and control response. System fittings and valve geometries may also influence flow and pressure behaviour, and thereby the accuracy of model predictions.

Then, the current model follows a lumped-parameter approach, which does not account for spatial variation within the tank. As a result, thermal stratification and localised heating effects are not simulated, although they may significantly affect tank pressure and venting. Furthermore, two-phase boiling at the liquid–wall interface is not included. Such phenomena can occur when relatively warm tank walls come into contact with cryogenic liquid hydrogen, resulting in rapid local vaporisation and additional venting. These effects are not captured in the current model and may lead to underestimation of transient thermal behaviour.

Further research is needed to establish certification and regulation for LH_2 refuelling, especially in relation to its integration with ground operations. Effective venting management remains a critical but insufficiently explored aspect. Additionally, the absence of pipelines in early-stage LH_2 infrastructure necessitates the use of intermediate storage, compressors, and high-pressure tanks, as outlined by Mangold et al. [21]. Future studies should also include a comprehensive analysis of compressor sizing and power requirements, as well as dynamic modelling of pumps, valves, and control systems to reflect realistic operational behaviour. Experimental validation under representative airport conditions is essential to confirm model predictions and support further standardisation.

In conclusion, this study demonstrates that LH_2 refuelling for future

Table 6
Results of the sensitivity analysis for the case study aircraft.

B. Results of the Sensitivity Analysis							
		t_{refuel} (s)	t_{refuel} (min)	t_{refuel}(−)	Jtr_{losses} (kg)	Jtrlosses (−)	Jtr_{losses} (%)
Tl,RT$_{t=0}$ (K)	19	1137	18.9	1.01	36.6	1.00	2.23
	20	1123	18.7	1.00	36.7	1.00	2.24
	20.86	1110	18.5	0.99	36.8	1.00	2.25
pvent,RT (bara)	1.4	1049	17.5	0.93	36.1	0.98	2.20
	2	1123	18.7	1.00	36.7	1.00	2.24
	2.5	1190	19.8	1.06	37.1	1.01	2.26
$\mathbf{q''RT}\left(\frac{W}{m^2}\right)$	5	1124	18.7	1.00	36.8	1.00	2.24
	7.5	1123	18.7	1.00	36.8	1.00	2.24
	10	1123	18.7	1.00	36.7	1.00	2.24
	12.5	1123	18.7	1.00	36.7	1.00	2.24
	15	1123	18.7	1.00	36.6	1.00	2.23
$\mathbf{L_{tr}}(m)$	5	966	16.1	0.86	36.9	1.01	2.25
	7.5	1048	17.5	0.93	36.8	1.00	2.24
	10	1123	18.7	1.00	36.7	1.00	2.24
	12.5	1196	19.9	1.06	36.6	1.00	2.23
	15	1263	21.0	1.12	36.5	0.99	2.23
RT tank material	Al5083	1123	18.7	1.00	36.7	1.00	2.24
	SS304	1124	18.7	1.00	36.8	1.00	2.24
$\mathbf{D_{tr}}$ (mm)	30	1123	18.7	1.00	36.7	1.00	2.24
	$140K = 11$	143	2.4	0.13	36.4	0.99	2.22
	$140K = 2.36$	133	2.2	0.12	36.5	1.00	2.23
$\mathbf{T_{w,}RT}$ (K)	$Tv,lt = 0$	1123	18.7	1.00	36.7	1.00	2.24
	30	1130	18.8	1.01	36.1	0.98	2.20
	40	1133	18.9	1.01	37.0	1.01	2.25
tw,RT (mm)	3	1124	18.7	1.00	36.7	1.00	2.24
	5	1123	18.7	1.00	36.7	1.00	2.24
	7	1123	18.7	1.00	36.7	1.00	2.24
Spray (%)	0	1123	18.7	1.00	36.7	1.00	2.24
	25	1118	18.6	1.00	32.6	0.89	1.99
	50	1114	18.6	0.99	30.6	0.83	1.86
	75	1111	18.5	0.99	28.5	0.78	1.74
	100	1108	18.5	0.99	25.6	0.70	1.56
Method	Serial	1123	18.7	1.00	36.7	1.00	2.24
	Parallel	1096	18.3	0.98	35.6	0.97	2.17
$\mathbf{p_{ST}}$ (bar_g)	3	1123	18.7	1.00	36.7	1.00	2.24
	4	964	16.1	0.86	35.9	0.98	2.19
Bombardier Q400 (PAX)	78	1285	21.4	1.14	42.3	1.15	2.58
	90	1123	18.7	1.00	36.7	1.00	2.24

regional aircraft is technically feasible within realistic time constraints. The presented model provides valuable insight into key design drivers and operational limitations, while also highlighting the importance of further research into more detailed simulations and infrastructure development. The results form a foundation for the continued advancement of safe, efficient, and certifiable LH_2 refuelling systems in aviation.

CRediT authorship contribution statement

L. ten Damme: Writing – original draft, Validation, Software, Methodology, Investigation, Formal analysis. **M. van Put:** Supervision, Resources, Project administration, Funding acquisition, Data curation, Conceptualization. **A. Gangoli Rao:** Writing – review & editing, Validation, Resources, Project administration, Methodology, Data curation, Conceptualization.

Declaration of competing interest

The authors declare that they have no known competing financial interests or personal relationships that could have appeared to influence the work reported in this paper.

References

[1] Boretti A, Castelletto S. NH3 prospects in combustion engines and fuel cells for commercial aviation by 2030. ACS Energy Lett 2022;7(8):2557–64. https://doi.org/10.1021/acsenergylett.2c00994.

[2] Proesmans P-J, Vos R. Comparison of future aviation fuels to minimize the climate impact of commercial aircraft. In: AIAA aviation 2022 forum; 2022. p. 3288.

[3] Lanz W. Module 1: hydrogen properties. In: Hydrogen fuel cell engines and related technologies; 2001.

[4] Ryan C, Philip SV. Airbus hydrogen plane with turboprop design gaining favor for zero emission jet [Online]. Available: https://www.bloomberg.com/news/articles/2021-02-11/airbus-turboprop-design-gaining-favor-as-first-hydrogen-plane#xj4y7vzkg. [Accessed 9 November 2023].

[5] Mar [Online]. Available, https://www.airbus.com/en/newsroom/stories/2021-03world-class-alternative-propulsion-testing-starts-here. [Accessed 9 November 2023].

[6] Jackson P. Jane's all the world's aircraft 2007-2008: Ninety-eighth year of issue. Jane's; 2007.

[7] James R. How long to refuel an airplane?. In: 15 most common planes; Oct. 2021 [Online]. Available: https://pilotteacher.com/how-long-to-refuel-an-airplane-15-most-commonplanes/. [Accessed 9 November 2023].

[8] Brouwer M, Srinivasan S. Proud to fly a turboprop: Q400 vs atr72. https://theflyingengineer.com/aircraft/proud-to-fly-a-turboprop-q400-vsatr72/. [Accessed 9 November 2023].

[9] [Online]. Available: https://bombardier.com/en/media/news/bombardier-delivers-first-90-seat-q400-aircraft-spicejet. [Accessed 9 November 2023].

[10] Knoblach A. Robust performance analysis for gust loads computation. Technische Universität Hamburg 2015. Ph.D. dissertation.

[11] Westenberger A. H2 technology for commercial aircraft. In: Proceedings of the advances on propulsion technology for high-speed aircraft. *Belgium*: *RTO, Rhode-Saint-Geneese*; 2007. p. 12–5.

[12] Airport hydrogen fuelling facility operations. Geneva, CH, Standard: International Organization for Standardization; Oct. 2004.

[13] Lemmon EW, Bell IH, Huber ML, McLinden MO. NIST standard reference database 23: reference fluid thermodynamic and transport Properties-REFPROP, version 10.0, National Institute of Standards and technology. https://doi.org/10.18434/T4/1502528; 2018. https://www.nist.gov/srd/refprop.

[14] Schröder M. Jul. 2022 [Online]. Available: https://www.now-gmbh.de/wp-content/uploads/2022/07/Wasserstoff-Vollversammlung_Wie-Wasserstoff-und-andere-Technologien-dieZukunft-der-Luftfahrt-veraendern_06.07.22.pdf. [Accessed 9 November 2023].

[15] de Boer PC, Wit Ad, van Benthem RC. Development of a liquid hydrogen-based fuel cell system for the hydra-2 drone. In: AIAA SCITECH 2022 Forum; 2022. p. 443.
[16] Onorato G. Fuel tank integration for hydrogen airliners. Delft University of Technology; 2021. MSc thesis.
[17] Vishnu S, Kuzhiveli BT. Effect of roughness elements on the evolution of thermal stratification in a cryogenic propellant tank. In: Low-Temperature technologies and applications. IntechOpen; 2021.
[18] [Online]. Available: http://hylium-industries.com/trailer (Accessed on 9/November/2023).
[19] Darr SR, Hartwig JW. Two-phase convection heat transfer correlations for liquid hydrogen pipe chilldown. Cryogenics 2020;105:102–999.
[20] [Online]. Available: https://www.durexindustries.com/electric-heaters/flange-immersion-heaters/6-inch-flange-nema-1-enclosure-no-thermostat (Accessed on 9/November/2023).
[21] Mangold J, Silberhorn D, Moebs N, Dzikus N, Hoelzen J, Zill T, Strohmayer A. Refueling of LH2 aircraft—assessment of turnaround procedures and aircraft design implication. Energies 2022;15(7):2475.
[22] Clean Aviation JU, FCHJU. A fact-based study of hydrogen technology, economics, and climate impact by 2050. In: Fuel cell and hydrogen joint undertaking. Boston, MA, USA: IGEM; 2020.